

# Cobalt–Cobalt Multiple Bonds in Homoleptic Carbonyls? $\text{Co}_2(\text{CO})_x$ ( $x = 5–8$ ) Structures, Energetics, and Vibrational Spectra

Joseph P. Kenny, R. Bruce King, and Henry F. Schaefer, III\*

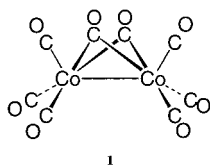
Center for Computational Quantum Chemistry, Department of Chemistry,  
University of Georgia, Athens, Georgia 30602

Received September 29, 2000

Homoleptic binary cobalt carbonyls with multiple cobalt–cobalt bonds have been examined theoretically using established levels of density functional methodology. These species include 19 structures ranging from the experimentally well characterized dibridged  $(\text{CO})_3\text{Co}(\text{CO})_2\text{Co}(\text{CO})_3$  to the proposed monobridged  $(\text{CO})_2\text{Co}(\text{CO})\text{Co}(\text{CO})_2$  structure with a formal quadruple bond. Consistent with experiment, three energetically low-lying equilibrium structures of  $\text{Co}_2(\text{CO})_8$  were found, of  $C_{2v}$  (dibridged),  $D_{3d}$  (unbridged), and  $D_{2d}$  (unbridged) symmetry. For  $\text{Co}_2(\text{CO})_8$ , the BP86 method predicts the dibridged structure to lie 3.7 kcal/mol below the  $D_{2d}$  structure and 6.3 kcal/mol below the  $D_{3d}$  structure. The  $D_{2d}$  and  $D_{3d}$  structures thus have the opposite energetic ordering of that deduced from experiment by Sweany and Brown. A satisfactory harmony between theoretical and experimental vibrational frequencies and IR intensities is found, although the  $D_{2d}$  and  $D_{3d}$  structures are essentially indistinguishable in this regard. For  $\text{Co}_2(\text{CO})_7$  the unbridged asymmetric structure suggested by Sweany and Brown is confirmed with the BP86 method, and with perhaps one exception the vibrational features agree well for theory and experiment. For  $\text{Co}_2(\text{CO})_6$  only one vibrational feature has been assigned from experiment, but this band ( $2011\text{ cm}^{-1}$ ) fits very well with BP86 predictions for the monobridged  $D_{2d}$  symmetry structure with a formal  $\text{Co}=\text{Co}$  triple bond. For the  $\text{Co}_2(\text{CO})_5$  molecule, for which no experimental results exist, the most interesting structure is the monobridged closed-shell singlet with a very short ( $2.17\text{ \AA}$ ) cobalt–cobalt bond, to which we assign a formal bond order of four. Potential energy distributions have been analyzed to identify the principal vibrations with cobalt–cobalt stretching contributions. The condensed phase Raman analysis by Onaka and Shriver of the Co–Co stretches for the three known isomers of  $\text{Co}_2(\text{CO})_8$  is remarkably consistent with the present predictions for the gas-phase species. Prospects for the synthesis of these and related dicobalt compounds are discussed.

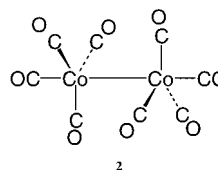
## Introduction

The simplest stable closed shell cobalt carbonyl is  $\text{Co}_2(\text{CO})_8$ , which is commercially available and has the well-known dibridged crystal structure of  $C_{2v}$  symmetry.<sup>1–3</sup>

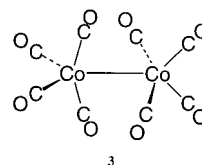


However, in solution the dibridged structure exists in competition with a second structure,<sup>4,5</sup> deduced to be the nonbridged  $D_{3d}$  geometry.

This equilibrium was the first experimentally established example of tautomerism in a polynuclear carbonyl. A third isomer of  $\text{Co}_2(\text{CO})_8$  was subsequently suggested from solution IR spectra.<sup>5–8</sup> Onaka and Shriver<sup>8</sup> concluded from solid and



solution phase Raman spectroscopy that the three distinct structures of  $\text{Co}_2(\text{CO})_8$  have Co–Co stretching vibrational frequencies of 235, 185, and  $159\text{ cm}^{-1}$ , respectively. From matrix isolation spectroscopy Sweany and Brown then concluded that the third structure IR features are in best accord<sup>9</sup> with a structure of  $D_{2d}$  symmetry.



Further spectroscopic<sup>10–15</sup> and computational<sup>16–24</sup> studies of  $\text{Co}_2(\text{CO})_8$  have added significantly to our understanding of this

(1) Sumner, G. G.; Klug, H. P.; Alexander, L. E. *Acta Crystallogr.* **1964**, *17*, 732.

(2) Leung, P. C.; Coppens, P. *Acta Crystallogr.* **1983**, *B39*, 535.

(3) Braga, D.; Grepioni, F.; Sabatino, P.; Gavezzotti, A. *J. Chem. Soc., Dalton Trans.* **1992**, 1185.

(4) (a) Noack, K. *Spectrochim. Acta* **1963**, *19*, 1925; *Helv. Chim. Acta* **47**, **1964**, 1064, 1554. (b) Bor, G. *Spectrochim. Acta* **14**, **1963**, 1209, 2065.

(5) Koelle, U. *Encyclopedia of Inorganic Chemistry*; King, R. B., Ed.; Wiley: Chichester, England, 1994; pp 733–747.

(6) Bor, G.; Noack, K. *J. Organomet. Chem.* **1974**, *64*, 367.

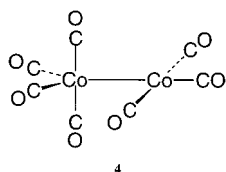
(7) Bor, G.; Dieler, U. K.; Noack, K. *J. Chem. Soc. Chem. Commun.* **1976**, 914.

(8) Onaka, S.; Shriver, D. F. *Inorg. Chem.* **1976**, *15*, 915.

(9) Sweany, R. L.; Brown, T. L. *Inorg. Chem.* **1977**, *16*, 415.

highly fluxional molecule. Bor et al.<sup>7</sup> even offer a sketch of the concentrations of the three  $\text{Co}_2(\text{CO})_8$  isomers as a function of temperature.

The removal of one or more carbonyls from  $\text{Co}_2(\text{CO})_8$  may result in systems with formal cobalt–cobalt multiple bonds, if the 18-electron rule is maintained. And, in fact, there is experimental evidence for  $\text{Co}_2(\text{CO})_7$  and perhaps also for  $\text{Co}_2(\text{CO})_6$ . Sweany and Brown<sup>10</sup> reported in 1977 that when a matrix of  $\text{Co}_2(\text{CO})_8$  is photolyzed with ultraviolet light, several bands may be assigned to  $\text{Co}_2(\text{CO})_7$ . The IR spectrum attributed to  $\text{Co}_2(\text{CO})_7$  contains no absorption characteristic of bridging carbonyl groups. Thus Sweany and Brown conclude that the structure of  $\text{Co}_2(\text{CO})_7$  is probably



Sweany and Brown<sup>10</sup> reported an additional band at  $2011\text{ cm}^{-1}$  that could not be readily assigned to  $\text{Co}_2(\text{CO})_8$ ,  $\text{Co}_2(\text{CO})_7$ , or any of the mononuclear species of cobalt. They suggest that the most likely candidate for this  $2011\text{ cm}^{-1}$  feature is  $\text{Co}_2(\text{CO})_6$ . Particularly relevant to the present research is the speculation of Sweany and Brown<sup>10</sup> that  $\text{Co}_2(\text{CO})_6$  possesses a  $\text{Co}\equiv\text{Co}$  triple bond. They further suggest a structure of  $D_{3d}$  symmetry for  $\text{Co}_2(\text{CO})_6$  with only two IR active modes in the CO stretching frequency region.

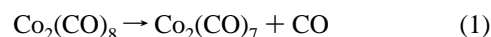
The purpose of this research is to examine the possibility of cobalt–cobalt multiple bonding in  $\text{Co}_2(\text{CO})_7$ ,  $\text{Co}_2(\text{CO})_6$ , and  $\text{Co}_2(\text{CO})_5$ . Invoking the 18-electron rule, one can readily see<sup>25,26</sup> the possibility of formal  $\text{Co}=\text{Co}$ ,  $\text{Co}\equiv\text{Co}$ , and  $\text{Co}^4\text{--Co}$  bonds, respectively for the above three molecular systems. In addition to the matrix isolation studies of Sweany and Brown,<sup>10</sup> other experimental approaches to these systems are now feasible. For example, Markin and Sugawara<sup>27</sup> have recently used mass spectrometric techniques to determine all nine of the dissociation energies for the successive removal of CO ligands from  $\text{Fe}_2$ –

$(\text{CO})_9^+$ . There is no obvious reason that the analogous experiments might not be carried out for  $\text{Co}_2(\text{CO})_8$ .

In addition to the  $\text{Co}_2(\text{CO})_7$  and  $\text{Co}_2(\text{CO})_6$  experiments of Sweany and Brown in 1977,<sup>10</sup> there is the 1993 report of Almond and Orrin<sup>14</sup> of photolysis of  $\text{Co}_2(\text{CO})_8$  in dioxygen matrices at 20 K. Almond and Orrin note that on photolysis the absorption features (at 2123, 2066, 2063, 1966, 1957, and  $1945\text{ cm}^{-1}$ ) assigned to the unsaturated  $\text{Co}_2(\text{CO})_7$  appear and grow. One final experimental paper that should be noted is the report of the coordinatively unsaturated  $\text{CoRh}(\text{CO})_7$  by Spindler et al.<sup>28</sup> This molecule, which is valence isoelectronic with  $\text{Co}_2(\text{CO})_7$ , turns out to be a yellow crystalline material<sup>29</sup> stable only below  $-65\text{ }^\circ\text{C}$  under  $\text{N}_2$ .

The theoretical papers by Thorn and Hoffmann<sup>16</sup> and by Dedieu et al.<sup>17</sup> provide lucid qualitative analyses of the bonding in  $\text{M}_2(\text{CO})_6$  systems, with attention to the present case  $\text{M} = \text{Co}$ . More recently, Bellagamba et al.<sup>19</sup> have reported extended Hückel studies of  $\text{Co}_2(\text{CO})_7$ .

The only density functional study of any of the unsaturated  $\text{Co}_2(\text{CO})_x$  systems is the year 2000 study by Barckholtz and Bursten<sup>24</sup> of  $\text{Co}_2(\text{CO})_7$ . They optimized the geometry of a structure similar to that proposed by Sweany and Brown (our structure **4** above). Further, Barckholtz and Bursten<sup>24</sup> predict the dissociation energy



to be  $32.3\text{ kcal/mol}$ , in perfect agreement with the 1980 Russian experimental result of Baev.<sup>30</sup> Barckholtz and Bursten also report good agreement with experiment for the first carbonyl dissociation energies of  $\text{Mn}_2(\text{CO})_{10}$  and  $\text{Fe}_2(\text{CO})_9$ .

## Theoretical Methods

Our basis set for C and O begins with Dunning's standard double- $\zeta$  contraction<sup>31</sup> of Huzinaga's primitive sets<sup>32</sup> and is designated (9s5p/4s2p). The double- $\zeta$  plus polarization (DZP) basis set used here adds one set of pure spherical harmonic d functions with orbital exponents  $\alpha_d(\text{C}) = 0.75$  and  $\alpha_d(\text{O}) = 0.85$  to the DZ basis set. For Co, in our loosely contracted DZP basis set, the Wachters' primitive set<sup>33</sup> is used but is augmented by two sets of p functions and one set of d functions, contracted following Hood et al.,<sup>34</sup> and designated (14s11p6d/10s8p3d). For  $\text{Co}_2(\text{CO})_8$ , there are 338 contracted Gaussian functions in the present DZP basis set.

Electron correlation effects were included by employing density functional theory (DFT) methods, which have been widely proclaimed as a practical and effective computational tool, especially for organometallic compounds. Among density functional procedures, the most reliable approximation is often thought to be the hybrid HF/DFT method using the combination of the three-parameter Becke exchange functional with the Lee–Yang–Parr nonlocal correlation functional known as B3LYP.<sup>35,36</sup> However, another DFT method, which combines Becke's 1988 exchange functional with Perdew's 1986 nonlocal correlation functional (BP86), was also used in the present paper for comparison.<sup>37,38</sup>

- (10) Sweany, R. L.; Brown, T. L. *Inorg. Chem.* **1977**, *16*, 421.
- (11) Abrahamson, H. B.; Frazier, C. C.; Ginley, D. S.; Gray, H. B.; Lilienthal, J.; Tyler, D. R.; Wrighton, M. S. *Inorg. Chem.* **1977**, *16*, 1554.
- (12) Ishii, M.; Ahsbals, H.; Hellner, E.; Schmid, G. *Ber. Bunsen-Ges. Phys. Chem.* **1979**, *83*, 1026.
- (13) Hanson, B.; Sullivan, M. J.; Davis, R. J. *J. Am. Chem. Soc.* **1984**, *106*, 251.
- (14) Almond, M. J.; Orrin, R. H. *J. Organomet. Chem.* **1993**, *444*, 199.
- (15) Brienne, S. H. R.; Markwell, R. D.; Barnett, S. M.; Butler, I. S.; Finch, J. A. *Appl. Spectrosc.* **1993**, *47*, 1131.
- (16) Thorn, D. L.; Hoffmann, R. *Inorg. Chem.* **1978**, *17*, 126.
- (17) Dedieu, A.; Albright, T. A.; Hoffmann, R. *J. Am. Chem. Soc.* **1979**, *101*, 3141.
- (18) Heijser, W.; Baerends, E. J.; Ros, P. *Faraday Symp. Chem. Soc.* **1980**, *14*, 211.
- (19) Bellagamba, V.; Ercoli, R.; Gamba, A.; Suffritti, G. B. *J. Organomet. Chem.* **1980**, *190*, 381.
- (20) Low, A. A.; Kunze, K. L.; MacDougall, P. J.; Hall, M. B. *Inorg. Chem.* **1991**, *30*, 1079.
- (21) Folga, E.; Ziegler, T. *J. Am. Chem. Soc.* **1993**, *115*, 5169.
- (22) Uffing, C.; Ecker, A.; Köppe, R.; Schnöckel, H. *Organometallics* **1998**, *17*, 2373.
- (23) Barckholtz, T. A.; Bursten, B. E. *J. Am. Chem. Soc.* **1998**, *120*, 1926.
- (24) Barckholtz, T. A.; Bursten, B. E. *J. Organomet. Chem.* **2000**, *596*, 212.
- (25) Ignatyev, I. S.; Schaefer, H. F.; King, R. B.; Brown, S. T. *J. Am. Chem. Soc.* **2000**, *122*, 1989.
- (26) Xie, Y.; Schaefer, H. F.; King, R. B. *J. Am. Chem. Soc.* **2000**, *122*, 8746.
- (27) Markin, E. M.; Sugawara, K. *J. Phys. Chem. A* **2000**, *104*, 1416.

- (28) Spindler, F.; Bor, G.; Dietler, U. K.; Pino, P. *J. Organomet. Chem.* **1981**, *213*, 303.
- (29) Horváth, I. T.; Bor, G.; Garland, M.; Pino, P. *Organometallics* **1986**, *5*, 1441.
- (30) Baev, A. K. *Russ. J. Phys. Chem.* **1980**, *54*, 1.
- (31) Dunning, T. H. *J. Chem. Phys.* **1970**, *53*, 2823.
- (32) Huzinaga, S. *J. Chem. Phys.* **1965**, *42*, 1293.
- (33) Wachters, A. J. H. *J. Chem. Phys.* **1970**, *52*, 1033.
- (34) Hood, D. M.; Pitzer, R. M.; Schaefer, H. F. *J. Chem. Phys.* **1979**, *71*, 705.
- (35) Becke, A. D. *J. Chem. Phys.* **1993**, *98*, 5648.
- (36) Lee, C.; Yang, W.; Parr, R. G. *Phys. Rev. B* **1988**, *37*, 785.
- (37) Becke, A. D. *Phys. Rev. A* **1988**, *38*, 3098.
- (38) Perdew, J. P. *Phys. Rev. B* **1986**, *33*, 8822.

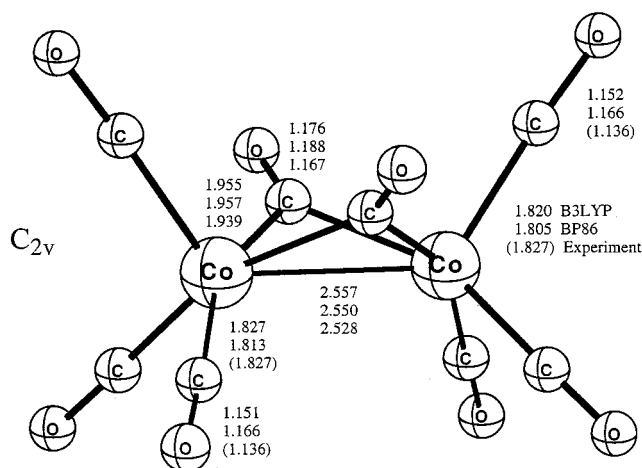


**Figure 1.** The dibridged structure of  $\text{Co}_2(\text{CO})_8$ , di- $\mu$ -carbonylhexacarbonyldicobalt. Experimental distances in parentheses reflect the fact that the crystal structure does not distinguish between the two different types of terminal carbonyls.

We fully optimized the geometries of all structures with both the DZP B3LYP and DZP BP86 methods. At the same levels we also report the vibrational frequencies by evaluating analytically the second derivatives of energy with respect to the nuclear coordinates. The corresponding infrared intensities are evaluated analytically as well. All the computations were carried out with the Gaussian 94 program<sup>39</sup> in which the fine grid (75 032) is the default for evaluating integrals numerically, and the tight ( $10^{-8}$  hartree) designation is the default for the SCF convergence.

The optimized geometries from these computations are depicted in Figures 1–19 with all bond distances given in angstroms.

## Results and Discussion

**A. Molecular Structures. I.  $\text{Co}_2(\text{CO})_8$ .** Figure 1 compares the present theoretical structures (DZP B3LYP and DZP BP86) with the known crystal structure.<sup>1–3</sup> Since the crystal structure does not distinguish between the two types of terminal carbonyls, a precise comparison between theory and experiment is not possible. B3LYP and BP86 suggest that the differences in terminal Co–C distances are 0.007 and 0.008 Å, respectively, with the four equivalent Co–C bonds being longer than the other two. For the terminal C–O distances, all 12 agree to within 0.001 Å.

Except for the Co–Co distance, the B3LYP structure provides better agreement than BP86 with experiment. The BP86 Co–Co distance is 0.022 Å longer than experiment, while B3LYP is longer by 0.029 Å. Folga and Ziegler<sup>21</sup> have earlier noted this problem, as their DFT Co–Co distance was 0.064 Å longer than experiment.

Figure 2 reports our B3LYP and BP86 geometries for the unbridged  $D_{3d}$  symmetry structure of  $\text{Co}_2(\text{CO})_8$ . This structure was earlier optimized by Folga and Ziegler<sup>21</sup> and by Barckholtz and Bursten<sup>24</sup> using the ADF program. The present DZP B3LYP and BP86 Co–Co distances (2.721 and 2.692 Å) are both longer than the 2.634 Å result of Folga and Ziegler. The theoretical studies agree that the known experimental dibridged  $C_{2v}$  structure has a much shorter (by 0.16 Å, B3LYP) Co–Co

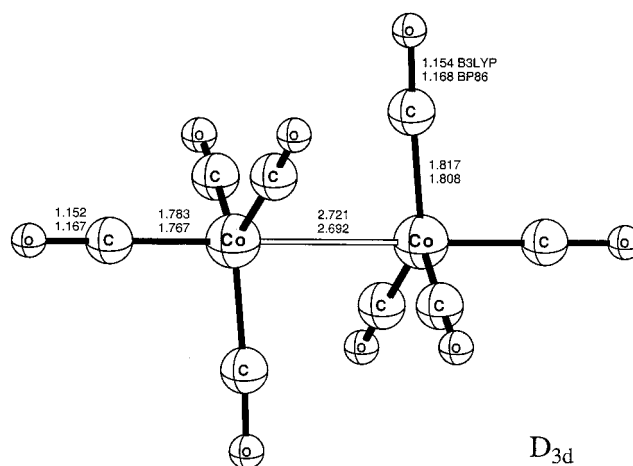


**Figure 2.** The  $D_{3d}$  unbridged structure of  $\text{Co}_2(\text{CO})_8$ , octacarbonyldicobalt.

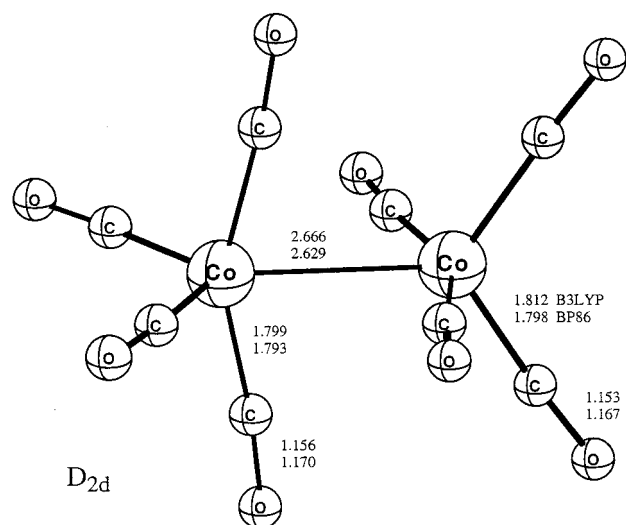


**Figure 3.** The  $D_{2d}$  unbridged structure of  $\text{Co}_2(\text{CO})_8$ , octacarbonyldicobalt.

distance than the  $D_{3d}$  structure, despite theoretical analysis<sup>20</sup> that reveals the absence of even a Co–Co single bond for the experimental  $C_{2v}$  structure. The shortest Co–C bond distance seen yet (1.783 Å, B3LYP) is predicted for the two axial distances in the unbridged  $D_{3d}$  structure (Figure 2).

The third  $\text{Co}_2(\text{CO})_8$  structure suggested by experiment<sup>5–9</sup> is seen in Figure 3. To our knowledge, this structure has not been optimized in previous theoretical studies. However, our DZP B3LYP and BP86 structures are similar to the qualitative sketch of  $\text{Mn}_2(\text{CO})_8$  given by Barckholtz and Bursten<sup>24</sup> in their Figure 4 (specifically their structure 5a). Our predicted Co–Co distance (2.666 Å, B3LYP) for the  $D_{2d}$  unbridged structure is intermediate between those for the experimental dibridged  $C_{2v}$  structure (2.557 Å) and the unbridged  $D_{3d}$  structure (2.721 Å).

All three  $\text{Co}_2(\text{CO})_8$  structures are predicted to be genuine minima with both the DZP B3LYP and DZP BP86 methods, consistent with the experimental conclusions from infrared studies.<sup>5–9</sup>

**II.  $\text{Co}_2(\text{CO})_7$ .** The qualitative structure **4** suggested by Sweany and Brown was investigated using both computational methods, and the results are seen in Figure 4. This structure is a genuine minimum with DZP B3LYP and very close to a genuine minimum with DZP BP86. The presence of four carbonyls on the left cobalt (Figure 4) would seem to restrict this structure to a cobalt–cobalt bond order no greater than one.

(39) Frisch, M. J.; Trucks, G. W.; Schlegel, H. B.; Gill, P. M. W.; Johnson, B. G.; Robb, M. A.; Cheeseman, J. R.; Keith, T.; Petersson, G. A.; Montgomery, J. A.; Raghavachari, K.; Al-Laham, M. A.; Zakrzewski, V. G.; Ortiz, J. V.; Foresman, J. B.; Peng, C. Y.; Ayala, P. Y.; Chen, W.; Wong, M. W.; Andes, J. L.; Replogle, E. S.; Gomperts, R.; Martin, R. L.; Fox, D. J.; Binkley, J. S.; Defrees, D. J.; Baker, J.; Stewart, J. J. P.; Head-Gordon, M.; Gonzalez, C.; Pople, J. A. *Gaussian 94*, Revision B.3; Gaussian Inc.: Pittsburgh, PA, 1995.

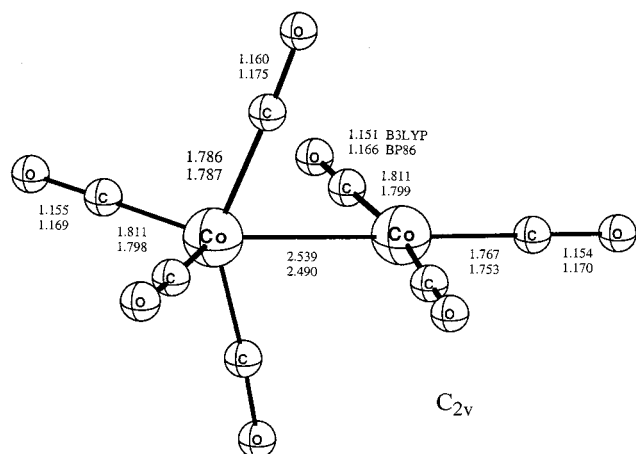


**Figure 4.** The unbridged structure of  $\text{Co}_2(\text{CO})_7$ , heptacarbonyldicobalt. This is the lowest energy structure of  $\text{Co}_2(\text{CO})_7$  found with the BP86 method. This is also the structure suggested by Sweany and Brown<sup>10</sup> based on their IR experiments.

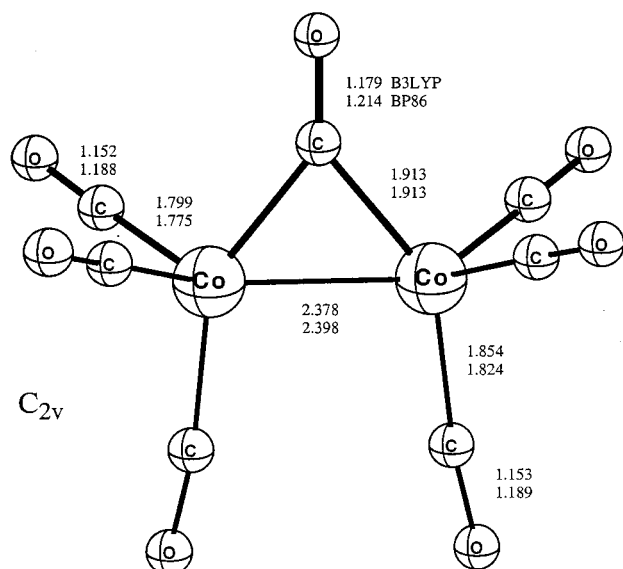


**Figure 5.** The singlet state  $C_{2v}$  monobridged structure of  $\text{Co}_2(\text{CO})_7$ ,  $\mu$ -carbonylhexacarbonyldicobalt.

The predicted Co–Co bond distances (B3LYP, 2.539 Å; BP86, 2.490 Å) are comparable to that observed experimentally (2.528 Å) for  $\text{Co}_2(\text{CO})_8$  and thus suggest the absence of multiple bonding. The four unique Co–C bond distances are predicted to be 1.767, 1.786, 1.811, and 1.811 Å, respectively, with the B3LYP method, which is quite reliable in this regard for the experimentally well-characterized  $\text{Co}_2(\text{CO})_8$ . The first two Co–C distances in  $\text{Co}_2(\text{CO})_7$  are interesting in that they are significantly shorter than the crystal structure terminal  $\text{Co}_2(\text{CO})_8$  distances, namely 1.827 Å. These short Co–C distances reflect the unsaturated nature of the  $\text{Co}_2(\text{CO})_7$  system.

With the monobridged structure, a formal double bond becomes possible for  $\text{Co}_2(\text{CO})_7$ . Figure 5 displays our predictions when such a  $\text{Co}_2(\text{CO})_7$  structure is confined to  $C_{2v}$  symmetry, the highest possible symmetry for such a structure. And indeed the predicted Co–Co distances are 2.378 Å (B3LYP) and 2.398 Å (BP86), much shorter than the 2.528 Å observed for  $\text{Co}_2(\text{CO})_8$ . Thus we are inclined to assign a Co=Co formal double bond to this structure. The two equivalent terminal Co–C distances are similar to that observed for  $\text{Co}_2(\text{CO})_8$ , but the four equivalent Co–C distances are shorter, namely 1.799 Å (B3LYP) or 1.775 Å (BP86). This monobridged

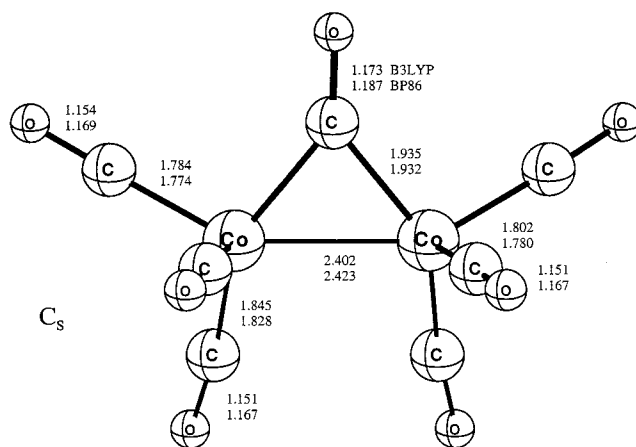


**Figure 6.** The  $C_s$  monobridged structure of  $\text{Co}_2(\text{CO})_7$ ,  $\mu$ -carbonylhexacarbonyldicobalt. This structure is predicted to lie about 1 kcal/mol below the higher symmetry monobridged structure seen in Figure 5.

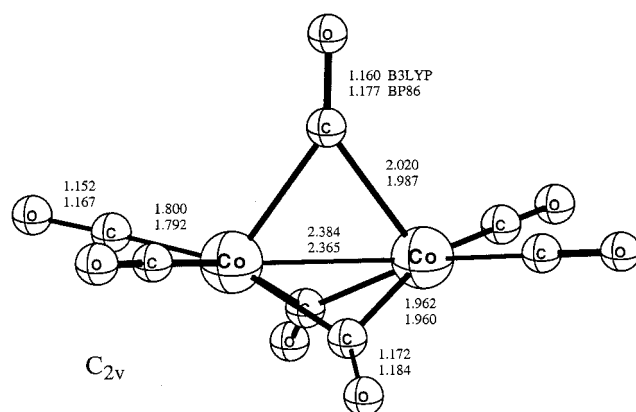


**Figure 7.** The tribridged structure of  $\text{Co}_2(\text{CO})_7$ , tri- $\mu$ -carbonyltetra-carbonyldicobalt.

$\text{Co}_2(\text{CO})_7$  structure will be seen to be energetically very close to a genuine minimum. We do predict a genuine minimum for a monobridged structure that is somewhat distorted with respect to Figure 5. This  $C_s$  symmetry structure is seen in Figure 6.

We have also predicted the equilibrium geometry of a tribridged  $\text{Co}_2(\text{CO})_7$  structure, and this is seen in Figure 7. As with the monobridged structure, the tribridged  $\text{Co}_2(\text{CO})_7$  possesses a much shorter cobalt–cobalt distance (2.384 Å, B3LYP; 2.365 Å, BP86). Thus we assign to this structure a formal Co=Co double bond. The bridging Co–Co distances (2.020 and 1.962 Å, B3LYP) for this  $\text{Co}_2(\text{CO})_7$  structure are somewhat longer than the 1.939 Å observed for  $\text{Co}_2(\text{CO})_8$ , suggesting some additional strain for this tribridged structure. Our tribridged structure will be seen to be quite close energetically to a genuine minimum.

A monobridged  $C_{2v}$  structure for the lowest triplet electronic state of  $\text{Co}_2(\text{CO})_7$  is reported in Figure 8. Unlike its double-bonded singlet counterpart (Figure 5), this triplet state displays a Co–Co bond distance (2.558 Å, B3LYP) representative of a formal single bond. We will see, however, that this triplet stationary point is not a genuine minimum. A triplet structure very close to a genuine minimum is presented in Figure 9. This lower energy triplet structure is semibridged with the B3LYP method and unsymmetrically monobridged with BP86. This  $C_s$  symmetry triplet state is the first case we have seen<sup>25,26</sup> among the binary homoleptic transition metal carbonyls where the B3LYP and BP86 methods give visibly different structural predictions.

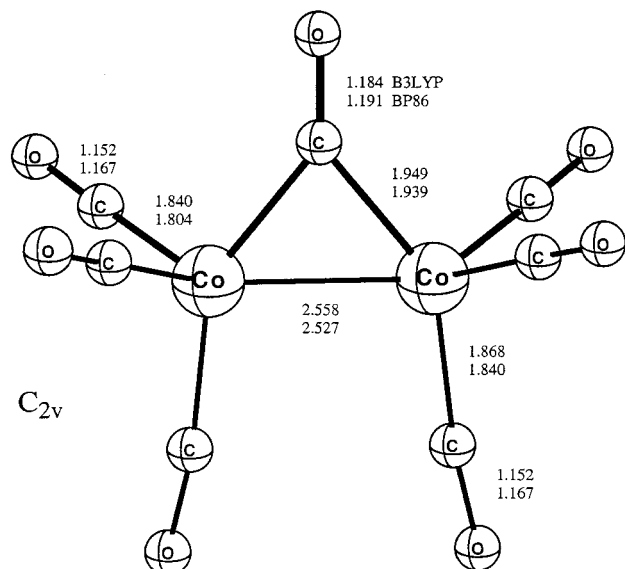


**Figure 8.** The triplet state monobridged structure of  $\text{Co}_2(\text{CO})_7$ ,  $\mu$ -carbonylhexacarbonyldicobalt.

**III.  $\text{Co}_2(\text{CO})_6$ .** Recall that in their laboratory infrared study Sweany and Brown postulated that  $\text{Co}_2(\text{CO})_6$ , for which they suggested an observed fundamental at  $2011\text{ cm}^{-1}$ , incorporates a  $\text{Co}\equiv\text{Co}$  triple bond. Our highest symmetry structure that might possess a  $\text{Co}\equiv\text{Co}$  triple bond is the doubly bridged  $D_{2h}$  structure shown in Figure 10. The predicted cobalt–cobalt distance (2.234 Å, B3LYP; 2.255 Å, BP86) is 0.3 Å shorter than the experimental Co–Co distance<sup>1–3</sup> for  $\text{Co}_2(\text{CO})_8$ . Thus we assign a formal triple bond to this  $D_{2h}$  structure of  $\text{Co}_2(\text{CO})_6$ . The four equivalent terminal Co–C distances (1.783 Å, B3LYP; 1.766 Å, BP86) are shorter than the 1.827 Å observed for  $\text{Co}_2(\text{CO})_8$ . A slightly distorted  $C_{2v}$  variant of this  $D_{2h}$  structure is shown in Figure 11.

As discussed by Hoffmann and co-workers,<sup>16,17</sup>  $\text{Co}_2(\text{CO})_6$  structures with 3-fold symmetry are expected to have triplet electronic ground states. Such a triplet electronic state should have a formal bond order no higher than two. Figures 12 and 13 show our predictions for the  $D_{3d}$  and  $D_{3h}$  structures, respectively, of  $\text{Co}_2(\text{CO})_6$ . Interestingly, the  $D_{3d}$  structure has a cobalt–cobalt distance only 0.037 Å longer (B3LYP) than the formally triple bonded  $D_{2h}$  symmetry structure. The eclipsed  $D_{3h}$  structure (Figure 13) is qualitatively similar to the  $D_{3d}$  geometry (Figure 12), but the former has a cobalt–cobalt distance 0.027 Å longer, consistent with simple repulsion arguments. It is probably best to think of the triplet 3-fold  $\text{Co}_2(\text{CO})_6$  as possessing a short formal double bond. An unsymmetrically dibridged triplet structure is shown in Figure 14.

Figure 15 shows the unbridged staggered structure of  $\text{Co}_2(\text{CO})_6$ , with bond distance 2.349 Å (BP86) most readily assigned to a formal double bond. Our final theoretical  $\text{Co}_2(\text{CO})_6$  structure is a planar  $D_{2h}$  symmetry unbridged structure (Figure 16). The predicted cobalt–cobalt distance for this structure is quite long, 2.773 Å for B3LYP and 2.705 Å for BP86, suggesting a single bond between the two equivalent 16-electron square planar Co sites.

**IV.  $\text{Co}_2(\text{CO})_5$ .** This is the only molecule considered in the present research for which there is no experimental evidence. Figure 17 presents our monobridged  $C_{2v}$  symmetry structure, which is either a genuine minimum or very close to a genuine minimum. The cobalt–cobalt distance is predicted to be remarkably short, namely 2.171 Å (B3LYP) or 2.173 Å (BP86). These distances are 0.386 Å (B3LYP) or 0.377 Å (BP86) shorter

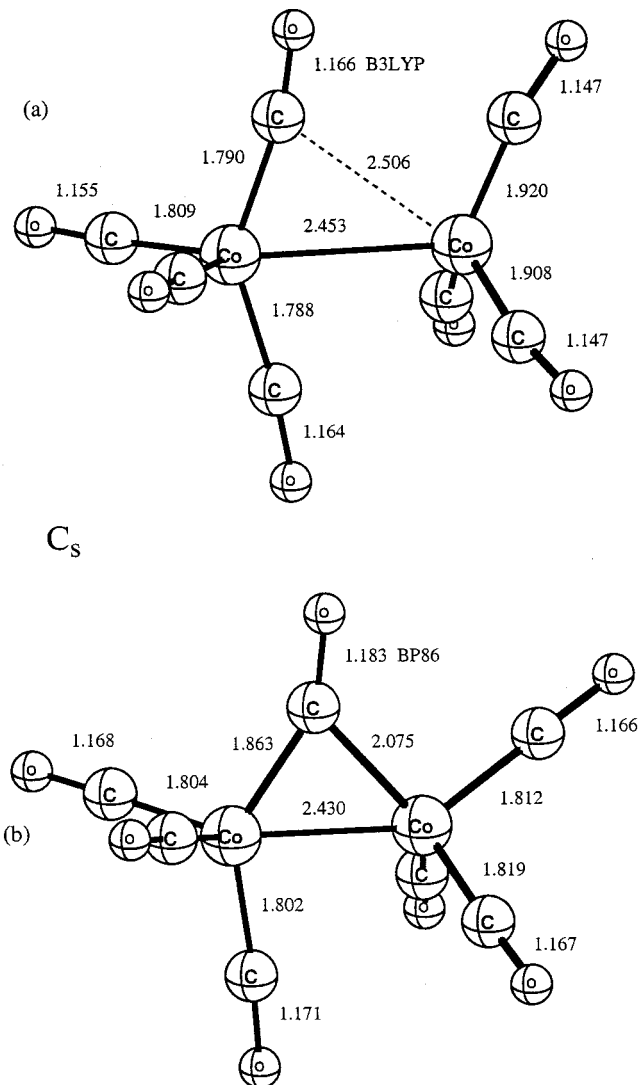


**Figure 9.** (a) The triplet state  $C_s$  semibridged B3LYP structure of  $\text{Co}_2(\text{CO})_7$ , heptacarbonyldicobalt; (b) the triplet state  $C_s$  monobridged BP86 structure of  $\text{Co}_2(\text{CO})_7$ ,  $\mu$ -carbonylhexacarbonyldicobalt.

than the analogous bond lengths for the known  $\text{Co}_2(\text{CO})_8$  structure. Thus it is reasonable to assign a formal  $\text{Co}^4\text{--Co}$  quadruple bond to this interesting structure. The Co–C bridging distance of 1.898 Å shows little sign of strain; it is predicted to be 0.041 Å shorter than that for the known  $\text{Co}_2(\text{CO})_8$  structure. The terminal Co–C distances are also shorter (by 0.041 Å, B3LYP; 0.057 Å, BP86) than those in the  $\text{Co}_2(\text{CO})_8$  crystal structure.<sup>1–3</sup>

Two triplet structures for  $\text{Co}_2(\text{CO})_5$  are seen in Figures 18 and 19. Both structures are tribridged, and they are obviously related. The higher symmetry  $D_{3h}$  structure relaxes to the lower symmetry  $C_{2v}$  structure. Both structures have Co–Co distances near 2.25 Å. With the two additional bridging carbonyls compared to Figure 17, it is clear that the two triplet structures have a cobalt–cobalt bond order significantly less than four.

In concluding our discussion of the relationship between bond distance and formal bond order, we want to emphasize the intrinsic tentativeness of any such discussion.<sup>40</sup> This is particularly so when comparisons are being made between structures involving varying numbers of bridging carbonyls.<sup>41</sup>

(40) Hoffmann, R. *Angew. Chem., Int. Ed. Engl.* **1982**, *21*, 711.

(41) Jemmis, E. D.; Pinhas, A. R.; Hoffmann, R. *J. Am. Chem. Soc.* **1980**, *102*, 2576.

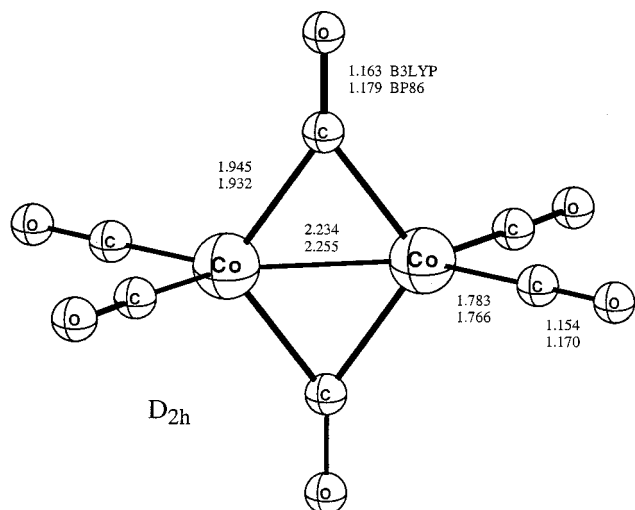


**Figure 10.** The high-symmetry  $D_{2h}$  dibridged structure of  $\text{Co}_2(\text{CO})_6$ , di- $\mu$ -carbonyltetracarbonyldicobalt.

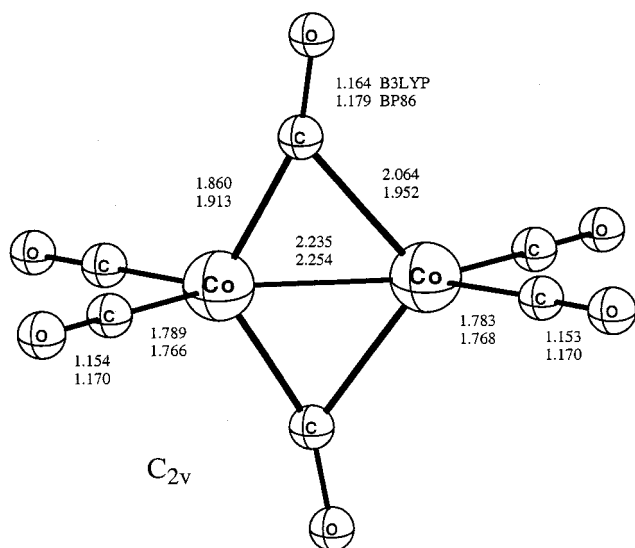
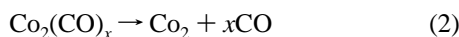
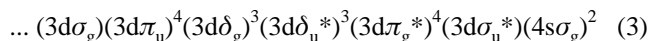


**Figure 11.** The singlet state distorted dibridged structure of singlet  $\text{Co}_2(\text{CO})_6$ , di- $\mu$ -carbonyltetracarbonyldicobalt.

**B. Thermochemistry.** There are several possible ways to evaluate the thermochemistry of the  $\text{Co}_2(\text{CO})_x$  structures predicted here. One such way, dissociation to metal dimer plus carbon monoxide molecules



is reported in Table 1. The electronic ground state of  $\text{Co}_2$  is not known from experiment, but both the B3LYP and BP86 methods predict<sup>42</sup> a  $^5\Sigma_g^+$  ground-state arising from the electron configuration



The first surprising result in Table 1 is how very close the three  $\text{Co}_2(\text{CO})_8$  structures lie energetically. Remember that the dibridged  $C_{2v}$  structure is the species for which the crystal structure has been determined experimentally. The DZP BP86 method does predict the dibridged structure to lie lowest energetically, but only 3.7 kcal/mol below the unbridged  $D_{2d}$

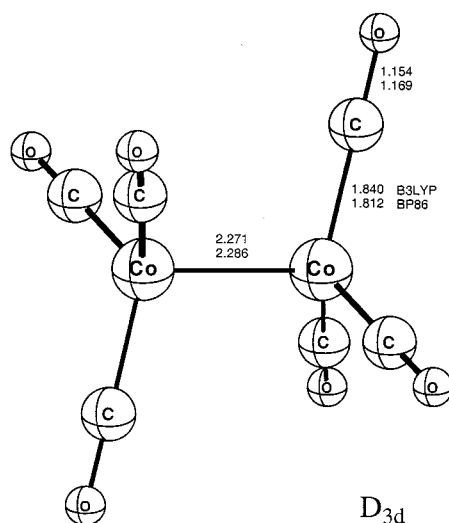


**Figure 12.** The triplet unbridged staggered structure of  $\text{Co}_2(\text{CO})_6$ , hexacarbonyldicobalt.

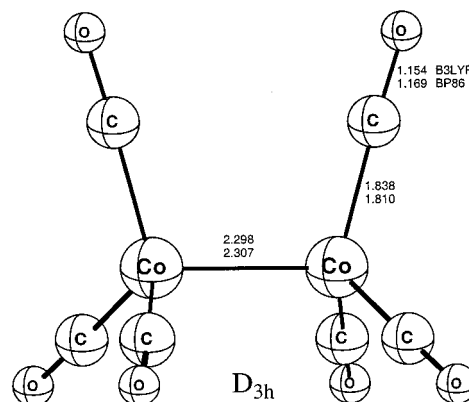


**Figure 13.** The triplet unbridged eclipsed structure of  $\text{Co}_2(\text{CO})_6$ , hexacarbonyldicobalt.

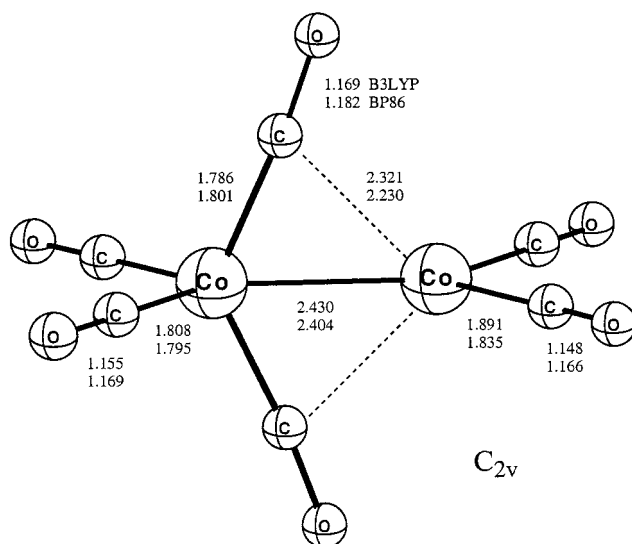


**Figure 14.** The triplet state partially dibridged structure of  $\text{Co}_2(\text{CO})_6$ , hexacarbonyldicobalt.

structure. Historically, the  $D_{2d}$  structure was the third to be observed by infrared techniques.<sup>5–8</sup> The unbridged  $D_{3d}$  structure, observed second,<sup>5</sup> is predicted by the DZP BP86 method to lie 6.3 kcal/mol above the dibridged structure. The latter result is in close agreement with the value 5.3 kcal/mol earlier predicted by Folga and Ziegler<sup>21</sup> using the ADF program.

(42) Barden, C. J.; Rienstra-Kiracofe, J. C.; Schaefer, H. F. *J. Chem. Phys.*, in press.

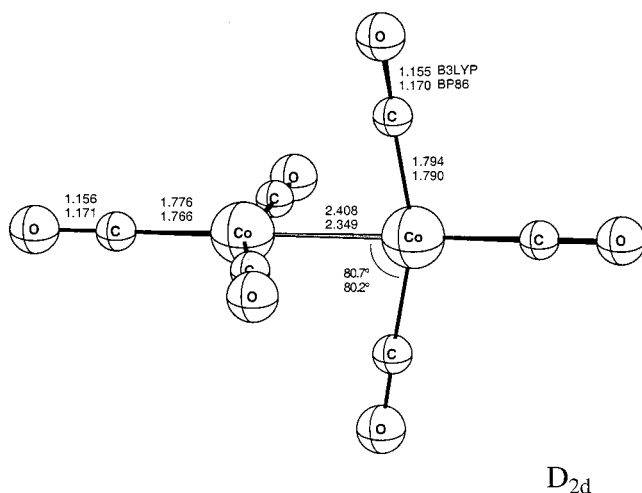


**Figure 15.** The unbridged staggered structure of  $\text{Co}_2(\text{CO})_6$ , hexacarbonyldicobalt.

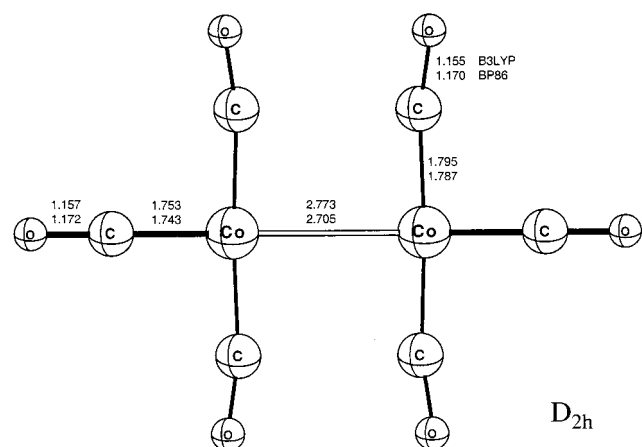


**Figure 16.** The unbridged eclipsed structure of  $\text{Co}_2(\text{CO})_6$ , hexacarbonyldicobalt.

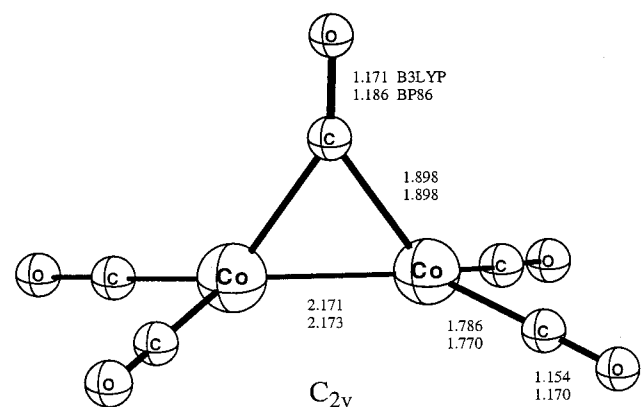


**Figure 17.** The monobridged structure of  $\text{Co}_2(\text{CO})_5$ ,  $\mu$ -carbonyltetracarbonyldicobalt.

With the DZP B3LYP method, the unbridged  $D_{2d}$  structure is predicted to lie lowest, with the dibridged  $C_{2v}$  structure only 0.5 kcal/mol higher in energy. The unbridged  $D_{3d}$  structure lies an additional 1.5 kcal/mol higher. For the complete dissociation of  $\text{Fe}_2(\text{CO})_9$ , our earlier research<sup>26</sup> showed the B3LYP method to give much better agreement with experiment than BP86. Thus, we are tempted to favor the B3LYP energetics over those predicted by BP86. What one can say fairly definitively is that theory shows that there are three distinct isomers of  $\text{Co}_2(\text{CO})_8$ ,

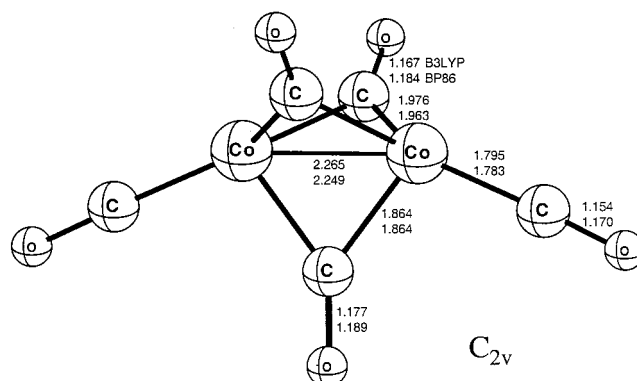


**Figure 18.** The tribridged singlet structure of  $\text{Co}_2(\text{CO})_5$ , tri- $\mu$ -carbonyldicarbonyldicobalt.

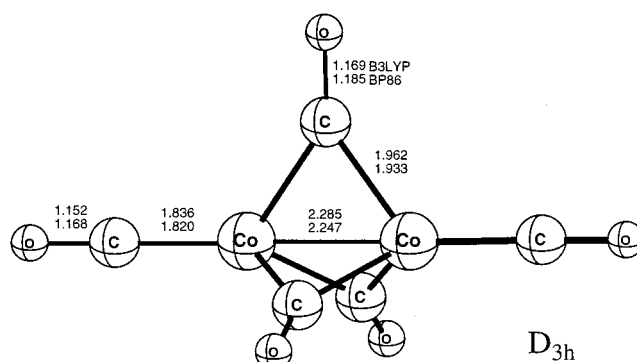


**Figure 19.** The tribridged triplet structure of  $\text{Co}_2(\text{CO})_5$ , tri- $\mu$ -carbonyldicarbonyldicobalt.

as apparently observed in the laboratory,<sup>5-8</sup> and that these isomers are nearly degenerate in the gas phase.

Sweany and Brown conclude from their observed IR spectra that at temperatures below 77 K, the order of free energies is

$$\text{I} (C_{2v}) < \text{II} (D_{3d}) < \text{III} (D_{2d}) \quad (4)$$

Sweany and Brown observe conversion from III to II to be extremely facile, a result nicely explained by the relatedness of our Figures 2 (their structure II) and 3 (their structure III). Finally, Sweany and Brown report that conversion of structure II (our  $D_{3d}$ ) to structure I (our  $C_{2v}$ ) occurs at 84 K with a free energy of activation of  $6.4 \pm 0.4$  kcal/mol. It is clear that the present BP86 predictions are in better agreement with Sweany and Brown's experimental energetics than are the B3LYP results.

For  $\text{Co}_2(\text{CO})_7$  the unbridged  $C_{2v}$  symmetry structure **4** recommended by Sweany and Brown<sup>10</sup> is predicted to be the lowest lying energetically by the DZP BP86 method. With BP86, there are several other structures in very close energetic proximity. Lying only 3.2 kcal/mol above the Sweany–Brown structure is the double-bonded tribridged  $C_{2v}$  symmetry structure of Figure 7. Only 1.0 kcal/mol higher is the monobridged minimum, also with a formal  $\text{Co}=\text{Co}$  double bond, seen in Figure 6.

The DZP B3LYP method predicts the semibridged triplet structure (Figure 9) to be the lowest energy isomer of  $\text{Co}_2(\text{CO})_7$ . With the B3LYP method, the only other structure within 16 kcal/mol of the semibridged triplet is the Sweany–Brown structure **4**, which lies 4.9 kcal/mol higher. It seems clear that convergent quantum mechanical methods, such as CCSD(T) with a large basis set, will be needed to theoretically provide definitive energetic predictions.

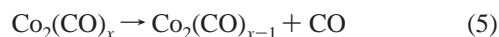
**Table 1.** Dissociation Energies (in kcal/mol) for  $\text{Co}_2(\text{CO})_x \rightarrow \text{Co}_2 + x\text{CO}$ 

<i>x</i>	formal central bond	spin	sym	Co–Co bond distance (Å)	no. of bridges	fig. no. in text	imaginary freq		B3LYP	per CO	BP86	per CO
							B3LYP	BP86				
5	$\text{Co}^4\text{--Co}$	singlet	$C_{2v}$	2.171	1	17	none	33i	159.3	31.9	243.5	48.7
	$\text{Co}\equiv\text{Co}$	triplet	$C_{2v}$	2.265	3	18	149i	none	150.1	30.0	244.0	48.8
	$\text{Co}\equiv\text{Co}$	triplet	$D_{3h}$	2.285	3	19	293i,240i,32i	106i,8i	151.5	30.3	242.2	48.4
6	$\text{Co}\equiv\text{Co}$	singlet	$D_{2h}$	2.234	2	10	204i	40i	202.5	33.8	297.0	49.5
	$\text{Co}\equiv\text{Co}$	singlet	$C_{2v}$	2.235	2	11	none	10i	203.3	33.9	297.0	49.5
	$\text{Co--Co}$	singlet	$D_{2d}$	2.408	0	15	18i,18i	53i,53i	200.4	33.4	285.7	47.6
	$\text{Co--Co}$	singlet	$D_{2h}$	2.773	0	16	46i,16i	47i,64i,41i,32i	181.0	30.2	265.1	44.2
	$\text{Co}=\text{Co}$	triplet	$D_{3d}$	2.271	0	12	266i,147i,47i	131i,75i	183.4	30.6	262.6	43.8
	$\text{Co}=\text{Co}$	triplet	$D_{3h}$	2.298	0	13	239i,183i,18i	110i,87i,18i	182.3	30.4	265.5	43.6
	$\text{Co--Co}$	triplet	$C_{2v}$	2.430	0	14	none	none	212.2	35.4	284.1	47.4
7	$\text{Co--Co}$	singlet	$C_{2v}$	2.539	0	4	none	39i	226.1	32.3	319.9	45.7
	$\text{Co}=\text{Co}$	singlet	$C_{2v}$	2.378	1	5	20i	26i	213.7	30.5	314.4	44.9
	$\text{Co}=\text{Co}$	singlet	$C_s$	2.402	1	6	none	none	214.5	30.6	315.7	45.1
	$\text{Co}=\text{Co}$	singlet	$C_{2v}$	2.384	3	7	31i,29i	30i	210.9	30.1	316.7	45.2
	$\text{Co--Co}$	triplet	$C_{2v}$	2.558	1	8	213i	686i	214.2	30.6	304.5	43.5
	$\text{Co--Co}$	triplet	$C_s$	2.453	0	9	16i	14i	231.0	33.0	313.9	44.8
8	$\text{Co--Co}$	singlet	$C_{2v}$	2.557	2	1	none	none	248.7	31.1	355.6	44.4
	$\text{Co--Co}$	singlet	$D_{3d}$	2.721	0	2	none	none	247.2	30.9	349.3	43.7
	$\text{Co--Co}$	singlet	$D_{2d}$	2.666	0	3	none	none	249.2	31.2	351.9	44.0

For  $\text{Co}_2(\text{CO})_6$  we again find the B3LYP and BP86 methods predicting rather different relative energies. B3LYP predicts the doubly semibridged  $C_{2v}$  triplet state (Figure 14) to lie lowest, followed 8.9 kcal/mol higher by the closed-shell doubly bridged  $C_{2v}$  symmetry structure (Figure 11). Recall that the doubly bridged structure was assigned a formal triple bond on the basis of geometrical considerations. With B3LYP, the latter  $C_{2v}$  geometry lies only 0.8 kcal/mol below the closely related  $D_{2d}$  structure seen in Figure 10. With the BP86 method the closed shell  $C_{2v}$  and  $D_{2d}$  structures have essentially the same energy and lie 12.9 kcal/mol below the doubly semibridged triplet. The staggered unbridged structure (Figure 15) is predicted to lie ~20 kcal/mol below the analogous eclipsed structure (Figure 16). The eclipsed unbridged and the other two  $\text{Co}_2(\text{CO})_6$  structures are predicted to lie significantly higher than the above-discussed structures with either the B3LYP or the BP86 method.

With the B3LYP method, the formal quadruple bond structure (monobridged Figure 16) is definitely the lowest lying in energy among  $\text{Co}_2(\text{CO})_5$  structures. With B3LYP, the triply bridged triplet structures (Figures 18 and 19) are predicted to lie 8–9 kcal/mol higher. However, with the BP86 method the three structures lie within 2 kcal/mol, and the tribridged  $C_{2v}$  triplet is predicted to be 0.5 kcal/mol below the monobridged closed-shell structure. Again one sees a situation in which convergent quantum mechanical techniques (e.g. large basis set CCSD(T) methods) are required to resolve the energetic differences between the B3LYP and BP86 results. Within 5 years such computations, with full geometry optimization, will be feasible, and we hope that new experiments for  $\text{Co}_2(\text{CO})_5$  will make such advanced theoretical studies a necessity.

On a per CO bond basis, the dissociation energies seen in Table 1 are rather uniform, ranging from 30.0 to 35.4 kcal/mol. With a method of viewing these data that is much more discriminating, Table 2 reports the thermochemistry in terms of the single carbonyl dissociation step



As noted in the Introduction, there is an experimental dissociation energy<sup>30</sup> for the extrusion of CO from  $\text{Co}_2(\text{CO})_8$ , namely 32.3 kcal/mol. The very same result was found in the theoretical study of Barckholtz and Bursten.<sup>24</sup> Our DZP BP86 result, 35.6 kcal/mol, is close to the above two results. However, our DZP B3LYP result, 18.2 kcal/mol, is much smaller. This

**Table 2.** Dissociation Energies (kcal/mol) for the Successive Removal of Carbonyl Groups from  $\text{Co}_2(\text{CO})_8$ <sup>a</sup>

	B3LYP	BP86
$\text{Co}_2(\text{CO})_8 \rightarrow \text{Co}_2(\text{CO})_7 + \text{CO}$	18.2	35.6
$\text{Co}_2(\text{CO})_7 \rightarrow \text{Co}_2(\text{CO})_6 + \text{CO}$	18.8	22.9
$\text{Co}_2(\text{CO})_6 \rightarrow \text{Co}_2(\text{CO})_5 + \text{CO}$	52.9	53.0

<sup>a</sup> All results reported here refer to the lowest energy structure of  $\text{Co}_2(\text{CO})_x$  optimized using the respective functional.

difference between B3LYP and BP86 is in part due to the fact that B3LYP predicts a triplet ground state for  $\text{Co}_2(\text{CO})_7$ , while BP86 predicts the singlet Sweany–Brown structure 4.

The predicted single carbonyl dissociation energy for  $\text{Co}_2(\text{CO})_7$  is 18.8 kcal/mol with B3LYP and 22.9 kcal/mol with BP86. In sharp contrast, the  $\text{Co}_2(\text{CO})_6$  dissociation process to  $\text{Co}_2(\text{CO})_5 + \text{CO}$  requires 52.9 kcal/mol at the B3LYP level and 53.0 kcal/mol with BP86. Thus  $\text{Co}_2(\text{CO})_6$  appears to be very stable with respect to extrusion of a carbonyl ligand.

**C. Vibrational Frequencies.** Harmonic vibrational frequencies have been evaluated for all 19 structures described above and are reported in Tables 3–7 in the text and Tables S1–S14 in the Supporting Information. The first question to be answered is which structures reported are minima. This is seen most quickly by reference to Table 1, in which the values of all predicted imaginary vibrational frequencies are reported. However, it must be emphasized that low magnitude imaginary vibrational frequencies are suspect with all currently available DFT methods. This is because the numerical integration procedures used in existing DFT methods have significant limitations. Thus, when one predicts an imaginary vibrational frequency of magnitude less than 100i  $\text{cm}^{-1}$ , the sober conclusion should be that there is a minimum of energy identical to or very close to that of the stationary point in question. Accordingly, we do not in general follow the imaginary eigenvector in search of a stationary point with no imaginary vibrational frequencies. In our earlier  $\text{Fe}_2(\text{CO})_x$  paper<sup>26</sup> we did reanalyze several such structures with very large integration grids, but the small imaginary vibrational frequencies remained. It is certainly desirable that future developments in DFT methodology would yield rock solid predictions for low fundamental vibrational frequencies. The molecules presented here would be splendid test cases for such new methodologies.

All three  $\text{Co}_2(\text{CO})_8$  structures are genuine minima with both of our DFT methods. For the dibridged structure, several



**Table 3.** Harmonic Vibrational Frequencies (in  $\text{cm}^{-1}$ ) and Infrared Intensities (in parentheses, in  $\text{km/mol}$ ) for Dibridged  $\text{Co}_2(\text{CO})_8$ ,  $C_{2v}$  Symmetry Di- $\mu$ -carbonylhexacarbonyldicobalt

	B3LYP DZP	BP86 DZP	experiment <sup>a</sup>
a <sub>2</sub>	27 (0)	24 (0)	
b <sub>1</sub>	38 (0)	37 (0)	
a <sub>1</sub>	41 (0)	41 (0)	
a <sub>2</sub>	67 (0)	65 (0)	
a <sub>1</sub>	70 (0)	69 (0)	
b <sub>2</sub>	76 (0)	73 (0)	
b <sub>1</sub>	78 (0)	76 (0)	
a <sub>1</sub>	88 (0)	84 (0)	
b <sub>2</sub>	91 (0)	87 (0)	
a <sub>2</sub>	93 (0)	95 (0)	
b <sub>1</sub>	97 (0)	92 (0)	
b <sub>2</sub>	110 (0)	107 (0)	
a <sub>1</sub>	112 (1)	107 (0)	
a <sub>2</sub>	204 (0)	214 (0)	
a <sub>1</sub>	225 (0)	223 (0)	
b <sub>2</sub>	242 (2)	239 (2)	
a <sub>2</sub>	313 (0)	319 (0)	
b <sub>1</sub>	343 (0)	340 (0)	
a <sub>2</sub>	352 (0)	350 (0)	
a <sub>1</sub>	361 (6)	361 (3)	
b <sub>1</sub>	367 (0)	369 (1)	
b <sub>2</sub>	373 (28)	373 (22)	
a <sub>1</sub>	404 (3)	407 (2)	
b <sub>1</sub>	406 (16)	404 (3)	
b <sub>2</sub>	411 (35)	433 (13)	
a <sub>2</sub>	428 (0)	442 (0)	
a <sub>1</sub>	432 (15)	452 (5)	
b <sub>1</sub>	439 (8)	447 (4)	
a <sub>1</sub>	450 (18)	468 (10)	
b <sub>2</sub>	452 (2)	477 (0)	
a <sub>2</sub>	468 (0)	471 (0)	
b <sub>1</sub>	491 (66)	491 (48)	
b <sub>2</sub>	528 (159)	524 (95)	
a <sub>1</sub>	529 (4)	523 (4)	
b <sub>2</sub>	533 (1)	533 (59)	
a <sub>1</sub>	544 (5)	544 (1)	
b <sub>1</sub>	559 (51)	553 (65)	
a <sub>2</sub>	566 (0)	563 (0)	
a <sub>1</sub>	588 (62)	577 (82)	
b <sub>2</sub>	666 (510)	642 (480)	
b <sub>1</sub>	1922 (833)	1869 (628)	1857 (4.2)
a <sub>1</sub>	1938 (273)	1878 (231)	1868 (2.7)
b <sub>2</sub>	2096 (11)	2011 (14)	2050 (1.9) ?
a <sub>2</sub>	2097 (0)	2010 (0)	
a <sub>1</sub>	2104 (1739)	2018 (1503)	
b <sub>1</sub>	2106 (1411)	2018 (1203)	2048 (7.8) ?
b <sub>2</sub>	2126 (1613)	2042 (1311)	2076 (10.0)
a <sub>1</sub>	2169 (18)	2079 (13)	2117 (0.1) ?

<sup>a</sup> Experimental IR frequencies are from ref 9. In parentheses are relative integrated intensities. Question marks indicate uncertainties stated by Sweany and Brown. Lower frequency features observed in solution and solid are discussed in the text.

fundamentals are known from matrix isolation experiments<sup>9</sup> and these are included in Table 3, which reports our theoretical predictions. The experimental results of Sweany and Brown<sup>9</sup> are particularly valuable in that they include relative integrated IR intensities. The strongest IR feature reported by Sweany and Brown is that appearing at  $2076 \text{ cm}^{-1}$ . This is clearly a terminal CO stretch and agrees satisfactorily with the three very intense IR fundamentals predicted by both B3LYP and BP86 methods. The other two features ( $1857$  and  $1868 \text{ cm}^{-1}$ ) unambiguously assigned by Sweany and Brown agree nicely with the intense b<sub>1</sub> and a<sub>1</sub> bridging carbonyl fundamentals predicted at  $1869$  and  $1878 \text{ cm}^{-1}$  by the BP86 method. The three assignments ( $2048$ ,  $2050$ ,  $2117 \text{ cm}^{-1}$ ) listed as questionable by Sweany and Brown have IR intensities (strong, medium, and weak, respectively) in plausible agreement with our theoretical predictions. Brienne

et al.<sup>15</sup> identify Sweany and Brown's weak  $2117 \text{ cm}^{-1}$  feature with  $2111 \text{ cm}^{-1}$  in the solid and identify it as an a<sub>1</sub> fundamental. This symmetry agrees with the theoretical predictions at  $2169 \text{ cm}^{-1}$  (B3LYP) or  $2079 \text{ cm}^{-1}$  (BP86).

Other vibrational features of the dibridged  $\text{Co}_2(\text{CO})_8$  have been observed in solid or solution phases. From Raman spectroscopy Onaka and Shriver<sup>8</sup> assign the Co–Co stretching fundamental at  $235 \text{ cm}^{-1}$ . We defer a discussion of this important fundamental to our detailed analysis (below) of the Co–Co force constants. Ishii et al.<sup>12</sup> nicely summarize the solid-state IR measurements in Table 2 of their paper. Ishii's strong IR feature at  $660 \text{ cm}^{-1}$  agrees nicely with our  $642 \text{ cm}^{-1}$  b<sub>2</sub> fundamental with IR intensity  $480 \text{ km/mol}$ . Weaker, but still substantial, theoretical IR fundamentals predicted at  $577 \text{ cm}^{-1}$  (a<sub>1</sub>,  $82 \text{ km/mol}$ ) and  $553 \text{ cm}^{-1}$  (b<sub>1</sub>,  $65 \text{ km/mol}$ ) agree well with the strong experimental features at  $578$  and  $549 \text{ cm}^{-1}$ . Perhaps the only puzzling aspect of the relationships between theory and experiment is the rather strong ( $159 \text{ km/mol}$  with B3LYP and  $95 \text{ km/mol}$  with BP86) theoretical IR b<sub>2</sub> fundamental predicted at  $528 \text{ cm}^{-1}$  with B3LYP and  $524 \text{ cm}^{-1}$  with BP86. This fundamental matches the observed feature at  $531 \text{ cm}^{-1}$ , but Ishii labels the latter feature "weak". The strongest theoretical IR feature below  $400 \text{ cm}^{-1}$  is the b<sub>2</sub> fundamental predicted at  $373 \text{ cm}^{-1}$  (intensity  $28 \text{ km/mol}$  with B3LYP,  $22 \text{ km/mol}$  with BP86), and this agrees well with the  $365 \text{ cm}^{-1}$  IR feature labeled medium intensity by Ishii.<sup>12</sup>

Taken as a whole, the comparisons between theory and experiment for vibrational frequencies suggest that the BP86 method is more reliable for  $\text{Co}_2(\text{CO})_8$  than is B3LYP. The single piece of experimental thermochemical data,<sup>30</sup> the endothermicity of  $\text{Co}_2(\text{CO})_8 \rightarrow \text{Co}_2(\text{CO})_7 + \text{CO}$ , also favors BP86 over B3LYP.

As noted in eq 4 above, Sweany and Brown concluded that the second lowest energy structure for  $\text{Co}_2(\text{CO})_8$  is the  $D_{3d}$  geometry seen in Figure 2. Accordingly, in Table 4, we attempt to relate the observed vibrational features of their structure II with our theoretical predictions for the  $D_{3d}$  equilibrium geometry. The agreement in Table 4 is plausible, with the three experimental features falling between the B3LYP and BP86 predictions. A similar identification of the observed IR features of structure III with our predicted  $D_{2d}$  harmonic vibrational frequencies is attempted in Table 5. Again the assignments are plausible with the experimental and theoretical IR intensities broadly consistent. Unfortunately, the fit is nearly as good if we assign Sweany and Brown's structure II with our  $D_{2d}$  structure and their structure III with our  $D_{3d}$  structure. This is not entirely surprising when one considers the structural similarity of the  $D_{3d}$  and  $D_{2d}$  structures, seen in Figures 3 and 4. Sweany and Brown seem to base their structural identifications of II ( $D_{3d}$ ) and III ( $D_{2d}$ ) on the fact that the  $D_{3d}$  structure gives rise to three IR-allowed fundamentals, while the  $D_{2d}$  structure yields four allowed IR fundamentals.

Turning to  $\text{Co}_2(\text{CO})_7$ , we follow Sweany and Brown<sup>10</sup> in our attempt to assign their six vibrational features to structure 4, the  $C_{2v}$  unbridged structure of  $\text{Co}_2(\text{CO})_7$ . To within  $2 \text{ cm}^{-1}$ , the same experimental vibrational features were observed by Almond and Orrin<sup>14</sup> in 1993 and similarly assigned to  $\text{Co}_2(\text{CO})_7$ . The experimental pattern of frequencies and IR intensities<sup>10,14</sup> does not match the theoretical predictions quite as well as is true for the three  $\text{Co}_2(\text{CO})_8$  structures. Both B3LYP ( $2097 \text{ cm}^{-1}$ ,  $2181 \text{ km/mol}$ ) and BP86 ( $2009 \text{ cm}^{-1}$ ,  $1881 \text{ km/mol}$ ) methods agree that the strongest IR feature is the b<sub>2</sub> CO stretching fundamental, and this could fit with Almond and Orrin's "strong" feature at  $2052 \text{ cm}^{-1}$ . Then the BP86 features at  $2009 \text{ cm}^{-1}$  (intensity  $678 \text{ km/mol}$ ) and  $2028 \text{ cm}^{-1}$  ( $835 \text{ km/mol}$ )

**Table 4.** Harmonic Vibrational Frequencies (in  $\text{cm}^{-1}$ ) and Infrared Intensities (in parentheses, in  $\text{km/mol}$ ) for the Unbridged Octacarbonyldicobalt,  $\text{Co}_2(\text{CO})_8$  of  $D_{3d}$  Symmetry

	B3LYP DZP	BP86 DZP	experiment <sup>a</sup>
$e_u$	37 (0)	34 (0)	
$a_{1u}$	48 (0)	46 (0)	
$e_g$	61 (0)	57 (0)	
$e_g$	81 (0)	74 (0)	
$e_u$	86 (0)	83 (0)	
$a_{1g}$	96 (0)	93 (0)	
$e_g$	96 (0)	92 (0)	
$e_u$	98 (0)	94 (0)	
$a_{2u}$	112 (2)	109 (2)	
$a_{1g}$	157 (0)	162 (0)	
$a_{2g}$	338 (0)	333 (0)	
$a_{1u}$	343 (0)	336 (0)	
$e_g$	352 (0)	351 (0)	
$e_u$	361 (8)	364 (4)	
$a_{2u}$	385 (73)	407 (39)	
$a_{1g}$	409 (0)	421 (0)	
$e_g$	448 (0)	450 (0)	
$a_{2u}$	459 (15)	472 (52)	
$e_u$	470 (56)	470 (29)	
$a_{1g}$	478 (0)	497 (0)	
$e_u$	489 (1)	496 (6)	
$e_g$	497 (0)	504 (0)	
$a_{2u}$	544 (315)	557 (227)	
$e_g$	558 (0)	556 (0)	
$e_u$	559 (67)	553 (78)	
$a_{1g}$	563 (0)	568 (0)	
$e_g$	2070 (0)	1989 (0)	
$a_{2u}$	2074 (3)	1995 (133)	2052 (1.9) ?
$e_u$	2087 (1906)	2006 (1605)	2026(4.8),2030(7.3)
$a_{1g}$	2102 (0)	2016 (0)	
$a_{2u}$	2121 (2099)	2045 (1343)	2074 (4.3)
$a_{1g}$	2169 (0)	2081 (0)	

<sup>a</sup> Experimental IR frequencies are from ref 9. In parentheses are relative integrated intensities. The question mark indicates an uncertainty stated by Sweany and Brown.

could fit with the “medium” intensity observed features at 2063 and 2066  $\text{cm}^{-1}$ . What does not seem to fit so well is the second strongest theoretical IR feature, namely the  $b_1$  CO stretching fundamental predicted at 2036  $\text{cm}^{-1}$  (1332  $\text{km/mol}$ ) by B3LYP and 1958  $\text{cm}^{-1}$  (1027  $\text{km/mol}$ ) by BP86. Both DFT methods predict this  $b_1$  frequency to be the lowest lying of the CO stretching fundamentals, by 21 or 22  $\text{cm}^{-1}$ , respectively. In contrast, Almond and Orrin<sup>14</sup> label their feature at 1945  $\text{cm}^{-1}$  as wm. However, we must note that in Sweany and Brown’s Figure 1, their observed feature at 1947  $\text{cm}^{-1}$  is reasonably prominent, and we would classify it as “medium” in IR intensity.

We should be quick to note that none of the other five theoretical structures for  $\text{Co}_2(\text{CO})_7$  does as satisfactorily in reproducing the IR features associated by Sweany and Brown with **4**. This is because all five of the remaining  $\text{Co}_2(\text{CO})_7$  structures have bridging carbonyls, leaving at least one fundamental falling below those observed by Sweany and Brown<sup>10</sup> and confirmed by Almond and Orin.<sup>14</sup> For example, perhaps the most interesting of these remaining  $\text{Co}_2(\text{CO})_7$  structures is the monobridged  $C_{2v}$  symmetry structure of Figure 5. The bridging CO stretch for Figure 5 is predicted (BP86) with strong IR intensity, at 1870  $\text{cm}^{-1}$ , too low to be assigned to any feature observed by Sweany and Brown. Thus, their identification of the seven IR features to their structure **4** seems convincing.

One of the most interesting aspects of Sweany and Brown’s paper concerns their observed feature at 2011  $\text{cm}^{-1}$ , which could not be assigned to any  $\text{Co}_2(\text{CO})_8$  or  $\text{Co}_2(\text{CO})_7$  species. They note “We might speculate that  $\text{Co}_2(\text{CO})_6$ , as a product of  $\text{Co}_2(\text{CO})_8$  photolysis, possesses a  $\text{Co}\equiv\text{Co}$  triple bond”. Our

**Table 5.** Harmonic Vibrational Frequencies (in  $\text{cm}^{-1}$ ) and Infrared Intensities (in parentheses, in  $\text{km/mol}$ ) for Unbridged  $\text{Co}_2(\text{CO})_8$ ,  $D_{2d}$  Symmetry Octacarbonyldicobalt

	B3LYP DZP	BP86 DZP	experiment <sup>a</sup>
$b_1$	32 (0)	33 (0)	
$e$	38 (0)	36 (0)	
$a_1$	63 (0)	66 (0)	
$b_2$	70 (1)	72 (1)	
$e$	71 (1)	61 (1)	
$a_2$	83 (0)	79 (0)	
$b_1$	85 (0)	82 (0)	
$e$	93 (0)	88 (0)	
$e$	98 (0)	96 (0)	
$a_1$	103 (0)	103 (0)	
$b_2$	121 (8)	120 (8)	
$a_1$	173 (0)	179 (0)	
$e$	330 (0)	329 (0)	
$a_2$	341 (0)	340 (0)	
$b_1$	347 (0)	347 (0)	
$e$	348 (1)	333 (1)	
$b_2$	403 (126)	426 (80)	
$a_1$	422 (0)	436 (0)	
$b_2$	442 (9)	453 (23)	
$e$	446 (2)	459 (1)	
$a_1$	455 (0)	467 (0)	
$b_2$	486 (43)	495 (26)	
$a_1$	496 (0)	502 (0)	
$e$	499 (10)	493 (15)	
$a_2$	536 (0)	563 (49)	
$b_1$	537 (0)	563 (49)	
$b_2$	541 (412)	538 (394)	
$e$	544 (74)	528 (0)	
$e$	569 (37)	551 (41)	
$a_1$	570 (0)	561 (0)	
$e$	2061 (336)	1982 (289)	1996 (2.0), 2002 (1.4)
$b_2$	2076 (30)	2002 (56)	2043 (1.8) ?
$a_1$	2083 (0)	2000 (0)	
$e$	2096 (1743)	2013 (1409)	2032 (4.9), 2035 (7.0)
$b_2$	2112 (1732)	2033 (1374)	2059 (5.2)
$a_1$	2168 (0)	2081 (0)	

<sup>a</sup> Experimental IR frequencies are from ref 9. In parentheses are relative integrated intensities. The question mark indicates an uncertainty stated by Sweany and Brown.

theoretical structure that fits this general description is the  $D_{2d}$  symmetry dibridged structure seen in Figure 10. And, indeed, the strongest predicted IR fundamental with both B3LYP (2419  $\text{km/mol}$ ) and BP86 (1846  $\text{km/mol}$ ) methods for this  $D_{2d}$  structure is predicted by BP86 at 2013  $\text{cm}^{-1}$ . Although the fit to experiment is essentially perfect, many a molecule has been incorrectly assigned on the basis of one observed vibrational feature. However, the fit is sufficiently suggestive to strongly encourage further experimental studies of  $\text{Co}_2(\text{CO})_6$ . Certainly, the technology of matrix isolation spectroscopy has significantly improved since Sweany and Brown’s pioneering 1977 experiments.<sup>10</sup>

The most important remaining vibrational question involves the critical matter of the cobalt–cobalt stretching frequencies. We have noted in the Introduction Onaka and Shriver’s conclusion from solid and solution phase Raman spectroscopy that the three observed  $\text{Co}_2(\text{CO})_8$  structures display cobalt–cobalt stretches at 229 (solid) or 235 (solution), 185, and 159  $\text{cm}^{-1}$ , respectively. Our analysis of cobalt–cobalt stretching was carried out in terms of the potential energy distributions (PEDs) evaluated using the remarkable program INTDER developed by Wesley D. Allen and co-workers. The most important results in this respect are reported in Table 8. There we predict the Co–Co stretching frequencies for the three distinct equilibrium geometries of  $\text{Co}_2(\text{CO})_8$  to be 225  $\text{cm}^{-1}$  (dibridged, Figure 1), 173  $\text{cm}^{-1}$  (unbridged  $D_{2d}$ , Figure 3), and 157  $\text{cm}^{-1}$  (unbridged

**Table 6.** Harmonic Vibrational Frequencies (in  $\text{cm}^{-1}$ ) and Infrared Intensities (in parentheses, in  $\text{km/mol}$ ) for Unbridged  $\text{Co}_2(\text{CO})_7$ , Heptacarbonyldicobalt, of  $C_{2v}$  Symmetry<sup>a</sup>

	experiment <sup>b</sup>			
	B3LYP DZP	BP86 DZP	Sweany & Brown <sup>10</sup>	Almond & Orrin <sup>14</sup>
b <sub>1</sub>	16 (0)	39i (0)		
b <sub>2</sub>	28 (0)	23 (0)		
a <sub>2</sub>	41 (0)	43 (0)		
b <sub>1</sub>	60 (0)	50 (1)		
a <sub>1</sub>	66 (1)	68 (1)		
b <sub>1</sub>	69 (1)	67 (0)		
b <sub>2</sub>	80 (1)	77 (1)		
a <sub>2</sub>	80 (0)	76 (0)		
a <sub>1</sub>	89 (0)	87 (0)		
b <sub>1</sub>	92 (0)	88 (0)		
b <sub>2</sub>	93 (0)	85 (0)		
b <sub>2</sub>	97 (0)	95 (0)		
a <sub>1</sub>	103 (4)	98 (5)		
a <sub>1</sub>	181 (0)	191 (0)		
b <sub>2</sub>	326 (0)	324 (0)		
b <sub>1</sub>	339 (1)	312 (1)		
a <sub>2</sub>	339 (0)	333 (0)		
a <sub>2</sub>	355 (0)	351 (0)		
b <sub>2</sub>	376 (6)	365 (3)		
b <sub>1</sub>	400 (5)	392 (2)		
a <sub>1</sub>	409 (57)	428 (39)		
a <sub>1</sub>	423 (5)	433 (6)		
b <sub>2</sub>	456 (14)	461 (3)		
a <sub>1</sub>	466 (20)	462 (67)		
b <sub>2</sub>	467 (7)	481 (4)		
a <sub>1</sub>	486 (1)	490 (0)		
b <sub>1</sub>	490 (5)	468 (0)		
a <sub>1</sub>	497 (29)	501 (8)		
b <sub>1</sub>	505 (1)	482 (8)		
a <sub>1</sub>	534 (285)	526 (192)		
a <sub>2</sub>	536 (0)	527 (0)		
b <sub>2</sub>	555 (115)	548 (103)		
b <sub>1</sub>	557 (76)	564 (58)		
b <sub>2</sub>	584 (7)	576 (10)		
a <sub>1</sub>	585 (62)	581 (70)		
b <sub>1</sub>	2036 (1332)	1958 (1027)	1947 (m)	1945 (wm)
a <sub>1</sub>	2057 (85)	1976 (123)	1955 (w)	1957 (m)
b <sub>2</sub>	2072 (48)	1987 (21)	1967 (s)	1966 (m)
a <sub>1</sub>	2095 (502)	2009 (678)	2053 (s)	2052 (s)
b <sub>2</sub>	2097 (2181)	2009 (1881)	2063 (s)	2063 (m)
a <sub>1</sub>	2106 (1401)	2028 (835)	2066	2066 (m)
a <sub>1</sub>	2167 (23)	2080 (18)	2123 (w)	2122 (wm)

<sup>a</sup> This is the lowest energy structure of  $\text{Co}_2(\text{CO})_7$  found with the BP86 method. <sup>b</sup> For the experiments of Sweany and Brown<sup>10</sup> we have crudely assigned intensities from their Figure 1.

$D_{3d}$ , Figure 2). The numerical agreement with Onaka and Shriver's experiments is either stunning or fortuitous, considering the fact that the theory refers to the gas phase and the experiments were done in condensed media.

Onaka and Shriver assign the  $235 \text{ cm}^{-1}$  Co–Co stretch to the dibridged structure, and this interpretation is confirmed here by theory. Onaka and Shriver do not attempt to distinguish structurally between the Co–Co stretches observed at 185 and  $159 \text{ cm}^{-1}$ . Our theoretical prediction is that the higher Co–Co stretch corresponds to the  $D_{2d}$  structure and the lower frequency to the  $D_{3d}$  structure.

Some comments on the predicted cobalt–cobalt stretching fundamentals of  $\text{Co}_2(\text{CO})_7$ ,  $\text{Co}_2(\text{CO})_6$ , and  $\text{Co}_2(\text{CO})_5$  are in order. In particular, for the structures plausibly assigned to formal double, triple, and quadruple bonds, does a Badger's rule correlation between bond distance and vibrational frequency exist? We note first that the total range in the theoretical metal–metal stretching frequencies is not great. However, our formal quadruple bond, the  $C_{2v}$  monobridged  $\text{Co}_2(\text{CO})_5$  structure (seen

**Table 7.** Harmonic Vibrational Frequencies (in  $\text{cm}^{-1}$ ) and Infrared Intensities (in parentheses in  $\text{km/mol}$ ) for Dibridged  $\text{Co}_2(\text{CO})_6$ ,  $D_{2h}$  Symmetry Di- $\mu$ -carbonyltetracobaltdicobalt

	B3LYP DZP	BP86 DZP	experiment <sup>a</sup>
b <sub>3u</sub>	204i (26)	40i (14)	
b <sub>2u</sub>	14 (0)	17 (0)	
a <sub>u</sub>	27 (0)	15i (0)	
b <sub>3g</sub>	65 (0)	65 (0)	
b <sub>1u</sub>	71 (1)	68 (1)	
b <sub>2u</sub>	71 (0)	70 (1)	
a <sub>g</sub>	79 (0)	78 (0)	
b <sub>2g</sub>	81 (0)	77 (0)	
b <sub>3u</sub>	86 (0)	92 (2)	
B <sub>1g</sub>	100 (0)	90 (0)	
b <sub>3u</sub>	162 (2)	210 (9)	
b <sub>2g</sub>	220 (0)	234 (0)	
a <sub>g</sub>	232 (0)	234 (0)	
b <sub>2g</sub>	301 (0)	285 (0)	
b <sub>3g</sub>	334 (0)	324 (0)	
a <sub>u</sub>	337 (0)	303 (0)	
b <sub>2u</sub>	339 (0)	337 (0)	
a <sub>g</sub>	383 (0)	396 (0)	
b <sub>1u</sub>	393 (11)	404 (4)	
b <sub>1g</sub>	405 (0)	402 (0)	
b <sub>3u</sub>	445 (0)	451 (8)	
b <sub>2u</sub>	463 (5)	448 (12)	
a <sub>g</sub>	494 (0)	512 (0)	
b <sub>1u</sub>	509 (43)	524 (29)	
b <sub>2u</sub>	509 (100)	531 (59)	
b <sub>2g</sub>	512 (0)	503 (0)	
b <sub>1g</sub>	521 (0)	543 (0)	
b <sub>3g</sub>	530 (0)	533 (0)	
b <sub>3u</sub>	553 (140)	564 (75)	
a <sub>g</sub>	586 (0)	592 (0)	
b <sub>1u</sub>	2002 (1460)	1919 (1165)	
a <sub>g</sub>	2013 (0)	1923 (0)	
b <sub>1g</sub>	2083 (0)	1988 (0)	
b <sub>2u</sub>	2089 (1810)	1995 (1529)	
b <sub>3u</sub>	2102 (2419)	2013 (1846)	2011
a <sub>g</sub>	2146 (0)	2050 (0)	

<sup>a</sup> Sweany and Brown<sup>10</sup> have assigned an experimental IR feature at  $2011 \text{ cm}^{-1}$  to  $\text{Co}_2(\text{CO})_6$ .

**Table 8.** Analysis of Vibrational Frequencies (in  $\text{cm}^{-1}$ ) Incorporating Cobalt–Cobalt Stretching Character<sup>a</sup>

$\text{Co}_2(\text{CO})_8$	$C_{2v}$	singlet dibridged	225 (84%), 450 (7%)
	$D_{3d}$	singlet unbridged	157 (73%), 96 (27%)
	$D_{2d}$	singlet unbridged	173 (74%), 103 (23%)
$\text{Co}_2(\text{CO})_7$	$C_s$	triplet unbridged	180 (83%), 339 (8%)
	$C_{2v}$	singlet monobridged	216 (85%), 457 (5%)
$\text{Co}_2(\text{CO})_6$	$C_{2v}$	triplet unbridged	198 (85%), 375 (7%)
	$D_{2h}$	singlet dibridged	232 (81%), 494 (10%)
$\text{Co}_2(\text{CO})_5$	$C_{2v}$	singlet monobridged	234 (77%), 574 (7%)

<sup>a</sup> The percentages reported reflect the analysis in terms of standard internal coordinates and their B3LYP resulting potential energy distributions (in parentheses, but neglected for those <5%). See Tables 3–8 and S1–S13 for complete listings of all vibrational frequencies and infrared intensities.

in Figure 17) with Co–Co distance 2.171 (B3LYP) or 2.173 Å (BP86), does display the highest metal–metal stretching fundamental, predicted at  $236 \text{ cm}^{-1}$  (BP86). Also, the second most important fundamental in terms of contribution from the Co–Co stretching force constant is at  $574 \text{ cm}^{-1}$  for the Co<sup>4</sup>–Co formal quadruple bond. This fundamental at  $574 \text{ cm}^{-1}$  (7% contribution from cobalt–cobalt stretch) is the highest frequency to appear in Table S14. Thus we conclude that there is a mild Badger's rule relationship between formal bond order/bond distance and metal–metal stretching vibrational frequency for the  $\text{Co}_2(\text{CO})_x$  species.

**D. Synthetic Prospects.** Figure 20 depicts the decarbonylation of the known  $\text{Co}_2(\text{CO})_8$  isomers to the  $\text{Co}_2(\text{CO})_x$  ( $x = 7$ ,

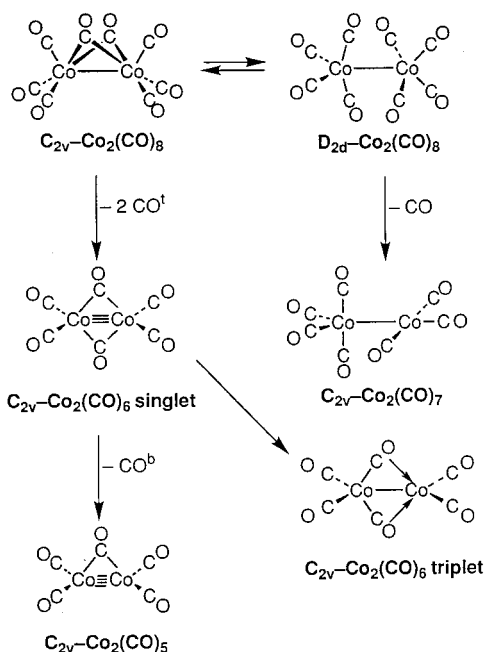


**Figure 20.** The decarbonylation processes converting the known  $\text{Co}_2(\text{CO})_8$  isomers to the  $\text{Co}_2(\text{CO})_x$  ( $x = 7, 6, 5$ ) isomers predicted by theory to correspond to the lowest energy minima.

6, 5) isomers predicted by the computations to correspond to the lowest energy minima. The lowest energy isomer of  $\text{Co}_2(\text{CO})_7$  is the unbridged isomer arising from loss of a carbonyl group from the unbridged isomer of  $\text{Co}_2(\text{CO})_8$ . The lowest energy singlet isomer of  $\text{Co}_2(\text{CO})_6$  arises from loss of a terminal CO group from each cobalt of the  $\text{C}_{2v}$  dibridged isomer of  $\text{Co}_2(\text{CO})_8$  with an increase in the formal cobalt–cobalt bond order from one to three and retention of the  $\text{C}_{2v}$  symmetry. This singlet isomer of  $\text{Co}_2(\text{CO})_6$  can distort to a likewise  $\text{C}_{2v}$  triplet isomer having geometry suggestive of semibridging CO groups functioning as four-electron donors (Figure 20) and thereby lowering the Co–Co bond order. In addition, loss of one of the two bridging CO groups from singlet  $\text{C}_{2v}\text{-Co}_2(\text{CO})_6$  generates the lowest energy  $\text{Co}_2(\text{CO})_5$  isomer, also of  $\text{C}_{2v}$  symmetry and formulated with a  $\text{Co}^4\text{-Co}$  quadruple bond.

Attempts to decarbonylate  $\text{Co}_2(\text{CO})_8$  in gram quantities by heating to give the  $\text{Co}_2(\text{CO})_x$  ( $x = 7, 6, 5$ ) isomers depicted in Figure 20 have all failed because of the facile conversion of  $\text{Co}_2(\text{CO})_8$  to  $\text{Co}_4(\text{CO})_{12}$  only slightly above room temperature.<sup>43</sup> Kinetics of this conversion of  $\text{Co}_2(\text{CO})_8$  to  $\text{Co}_4(\text{CO})_{12}$  indicates a rate law which is second order in  $[\text{Co}_2(\text{CO})_8]$  and inverse order in CO pressure ranging from  $-2$  in heptane to  $-4$  in toluene.<sup>44</sup> This rate law has been interpreted to suggest a preequilibrium

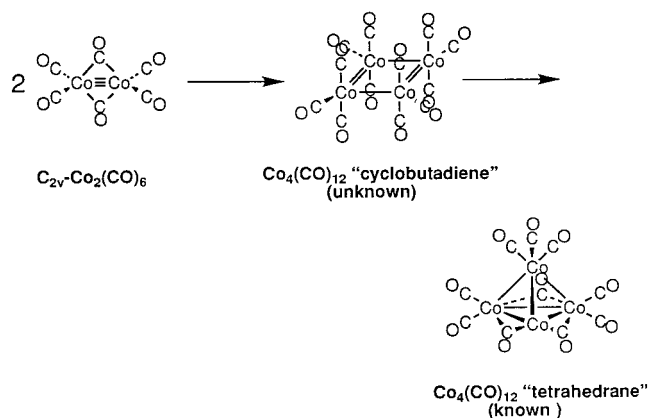


**Figure 21.** Dimerization of  $\text{C}_{2v}\text{-Co}_2(\text{CO})_6$  to the known "tetrahedrane"  $\text{Co}_4(\text{CO})_{12}$  through a "cyclobutadiene" intermediate.

involving the double decarbonylation of  $\text{Co}_2(\text{CO})_8$  to  $\text{Co}_2(\text{CO})_6$  via  $\text{Co}_2(\text{CO})_7$ , followed by dimerization of  $\text{Co}_2(\text{CO})_6$  to  $\text{Co}_4(\text{CO})_{12}$ . These observations suggest that  $\text{Co}_2(\text{CO})_6$  is unstable with respect to dimerization, leading ultimately to a tetrahedrane derivative, possibly through a cyclobutadiene-type intermediate (Figure 21) similar to the dimerization of certain acetylenes.

Matrix isolation infrared  $\nu(\text{CO})$  spectra suggest<sup>10</sup> that the low-temperature photochemical decomposition of  $\text{Co}_2(\text{CO})_8$  in argon matrices leads to an unbridged isomer of  $\text{Co}_2(\text{CO})_7$ , but this species has not been synthesized in macroscopic amounts. However, the closely related crystalline material  $\text{CoRh}(\text{CO})_7$  is known<sup>28</sup> and exhibits an infrared spectrum with no  $\nu(\text{CO})$  frequencies below  $1950 \text{ cm}^{-1}$ , suggesting the absence of bridging CO groups.<sup>29</sup> The thermal instability (above  $-65 \text{ }^\circ\text{C}$ ) of  $\text{CoRh}(\text{CO})_7$  has so far prevented determination of its structure by X-ray diffraction methods. Neither  $\text{Rh}_2(\text{CO})_8$  (ref 45) nor  $\text{CoRh}(\text{CO})_8$  (ref 29) analogous to  $\text{Co}_2(\text{CO})_8$  appears to be stable under ambient conditions, suggesting that substitution of Rh for Co is a possible approach to the synthesis of binuclear carbonyls of group 9 metals with M/Co ratios below 4.

**Acknowledgment.** This research was supported by the National Science Foundation, Grant CHE-9815397. We thank Dr. Yaoming Xie for many helpful discussions and for much computational assistance.

**Supporting Information Available:** Tables S1–S14, which give vibrational frequencies and infrared intensities for structures for which there is no claim of experimental identification. This material is available free of charge via the Internet at <http://pubs.acs.org>.

IC001279N

(43) Mond, L.; Hirtz, H.; Cowap, M. D. *J. Chem. Soc.* **1910**, 798; Ercoli, R.; Chini, P.; Massimauri, M. *Chim. Ind. (Milan)* **1959**, *41*, 132.

(44) Ungváry, F.; Markó, L. *Inorg. Chim. Acta*, **1970**, *4*, 324; Ungváry, F.; Markó, L. *J. Organomet. Chem.* **1974**, *71*, 283.

(45) Whyman, R. *Chem. Commun.* **1970**, 1194.